Observation of particle pairing in a two-dimensional plasma crystal

S. K. Zhdanov,* V. Nosenko, H. M. Thomas, and G. E. Morfill
Max Planck Institute for Extraterrestrial Physics, D-85741 Garching, Germany

L. Couëdel
CNRS, Université d'Aix-Marseille, PIIM UMR 7345, 13397 Marseille Cedex 20, France
(Received 5 June 2013; revised manuscript received 29 October 2013; published 12 February 2014)

The observation is presented of naturally occurring pairing of particles and their cooperative drift in a two-dimensional plasma crystal. A single layer of plastic microspheres was suspended in the plasma sheath of a capacitively coupled radio-frequency discharge in argon at a low pressure of 1 Pa. The particle dynamics were studied by combining the top-view and side-view imaging of the suspension. Cross-analysis of the particle trajectories allowed us to identify naturally occurring metastable pairs of particles. The lifetime of pairs was long enough for their reliable identification.

DOI: 10.1103/PhysRevE.89.023103 PACS number(s): 52.27.Lw, 52.27.Gr, 36.40.Mr

I. INTRODUCTION

A weakly ionized gas comprising dust or other fine solid particles is known as a complex, or dusty, plasma [1–3]. In experimental studies of complex plasmas the particle size is of a few nanometers to tens of microns. Immersed into a plasma, the particles charge up and interact with each other. It is a well-established fact that complex plasmas are able to self-organize, forming a highly ordered structure, *plasma crystal*, when the mutual interparticle interaction energy exceeds significantly their kinetic energy [4]. In the presence of gravity, a single-layer, or 2D, plasma crystal can form. The past two decades of studies showed that plasma crystals can be exploited as a useful tool to model or at least mimic at a kinetic level many phenomena as diverse as particle and energy transport in solids and liquids, crystal layer plasticity, phase and structural transitions, etc. [1,2].

In plasma crystals, as in any other crystalline structures, point defects and dislocations are ubiquitous [5,6]. They may present an obstacle to performing some delicate experiments. Additionally, plasma crystals sometimes suffer from the presence of extra particles [7], which do not belong to the crystalline structure and can cause local instabilities and disturb the lattice. (Such particles are sometimes called "unstable," "anomalous," etc., or even, addressing their position in the flow of ions with respect to a particle layer, "upstream" or "downstream"; see, e.g., Ref. [8].) On the other hand, they can be successfully used, as the studies performed recently have shown, as an active agent in the plasma crystal heating experiments [9,10], as a convenient practical diagnostic tool allowing to test in the simplest way the complex plasma elasticity modules [11–13], or as a probe of the plasma electric field distribution [14].

The particles that constitute the main lattice of a crystal are called *intralayer* particles. This terminology is also used in the granular media [15] and colloidal [16] physics. The particles located between the layers in multilayer crystals [9,17] are naturally called the *interlayer* particles [16,17].

The dynamics of interlayer particles are cardinally different from those of the intralayer particles. For example, the dynamics of a single second-layer Delrin particle [15] free to move on top of a granular dimer lattice, or the cooperative permeation of string-like clusters in colloids of rods [16], reveal unusual features. In plasma crystal studies, the particles moving in a plane above a single-layer plasma crystal (they were termed *upstream* particles in Ref. [8]) reveal elements of "strange kinetics" [18], such as channeling and leapfrog motion [8].

The interaction of an upstream particle with the plasma crystal located beneath it (downstream of the ion flow) is strongly influenced by the ion wake. An ion wake is a build-up of positive space charge created behind a negatively charged particle by a flow of ions past it [19–27]. Therefore, the wake-mediated interaction of an upstream particle with the plasma crystal is attraction-dominated [8].

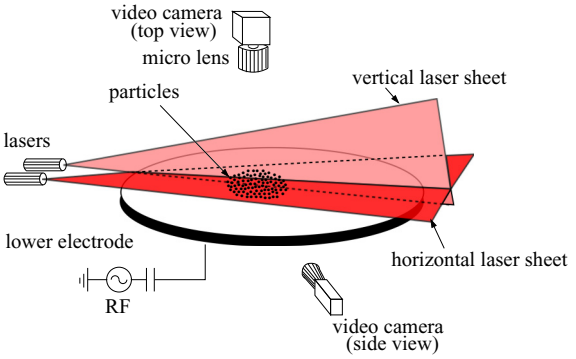

FIG. 1. (Color online) Sketch of the experimental setup. Plastic microspheres are confined in a stable single layer above the lower rf electrode in a capacitively coupled rf discharge in argon (the top ring-shaped grounded electrode is not shown here). The particle illumination system consists of two orthogonal laser sheets with different wavelengths. The particles are imaged from the top and from the side by two digital cameras equipped with narrow-band interference filters to admit only the respective wavelengths. This setup enables simultaneous recording of the in-plane and out-of-plane particle motion.

*zh@mpe.mpg.de

A delicate repulsion-attraction balance can result in a strong correlation—*pairing* of the upstream particle with a neighboring intralayer one. To some extent, this kind of pairing resembles the famous Cooper electron pairs when the electron-phonon interactions produce a strong preference for singlet zero momentum electron pairs [28]. The idea of a *dust molecule* proposed in Refs. [29,30] was later realized experimentally demonstrating that two (different) particles can be bound by attractive ion-wake-mediated net forces into a vertically aligned pair [31–33]. (The in-plane interaction of identical particles is repulsive for all interparticle separations [34].) Subsequently, the dust molecules were a subject of many detailed investigations, e.g., Ref. [35]; for review, see Ref. [36]. Vertical pairing of two identical particles in the sheath of a radio-frequency (rf) discharge has been studied in Ref. [20].

In this paper, we report on the first direct observation of spontaneous particle pairing and dragging occurring under natural conditions in a 2D complex plasma. Neither a torque, as in the "rotating wall" technique of Refs. [27,37], nor a laser beam, as in the laser-dragging experiment of Ref. [21], nor any other method of external manipulation has been used. Using paired particles as a probe of the mutual interparticle interaction is one more possibility that is briefly discussed in this paper.

II. EXPERIMENTAL PROCEDURE

The experiments were performed in a modified version of the Gaseous Electronics Conference (GEC) rf reference cell [24] using argon at a pressure of 1 Pa and melamine-formaldehyde microspheres with a diameter of $9.19 \pm 0.14\,\mu$m, a mass of $m = 6.1 \times 10^{-13}$ kg, and a weight of $mg = 6$ pN, where g is the free-fall acceleration on earth. A stylized sketch of the experimental setup is shown in Fig. 1. A weakly ionized plasma is generated by applying a forward rf power of 15 W at 13.56 MHz to the lower disk-shaped rf electrode (corresponding to the self-bias voltage $V_{dc} = -124$ V). The microparticles, introduced into the plasma using a dispenser, formed a stable monolayer confined in the plasma sheath above the rf electrode.

Optical ports and windows at the top and the side of the chamber provide access for the laser illumination and recording systems. Two digital cameras (a Photron FASTCAM 1024 PCI operating at 250 frames per second (fps) and a Basler Ace ACA640-100GM at 103.56 fps) recorded the microparticle positions and their dynamics and provided top-view (TV) and side-view (SV) snapshot sequences subjected further to a standard particle tracking technique [38,39]. Side-view imaging is usually used in 2D plasma crystal experiments only as a complementary diagnostic. In the present study, we relied on it for our main results. Therefore, we first verified the side-view data, using the fluctuation spectra of the particle out-of-plane motion, see Fig. 2, as a cross-check. Additionally, the side-view camera was used to verify that our experiments were carried out with a (dominantly) single layer of particles.

III. COMPLEX PLASMA PARAMETERS

The plasma crystal parameters were evaluated using a well-developed method based on the particle-tracking technique

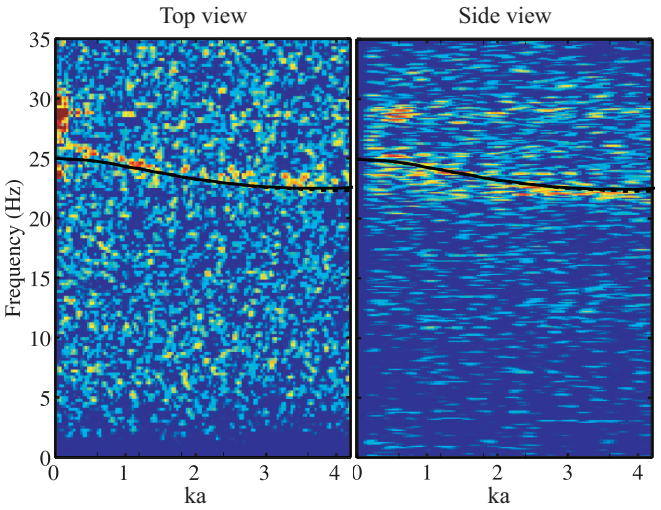

FIG. 2. (Color) Fluctuation spectra of the out-of-plane particle velocity in a 2D plasma crystal. The spectra were calculated from the top-view experimental movies (using the image intensity-sensitive analysis technique [13,24,46], left panel) or directly from the side-view movies (right panel). The intensities of the spectra are in arbitrary units (the logarithmic scale spans over two decades). The theoretical dispersion relations [41] for the two main crystallographic directions (solid and dashed lines) are very close to each other. A reasonably good agreement of the theoretical and experimental results is evident. The intercept of the out-of-plane phonon spectrum with the frequency axis gives the vertical confinement parameter f_v; see Table I. An unrelated excitation at about 29 Hz is separated from the spectrum by a gap of about 3–5 Hz.

[39]. The lattice constant a was obtained from the first peak of the pair correlation function $g(r)$. The neutral gas damping rate was estimated to be $\gamma_E \simeq 1.2$ s^{-1} [40]. The small value of γ_E (compared to characteristic frequency of the plasma crystal)

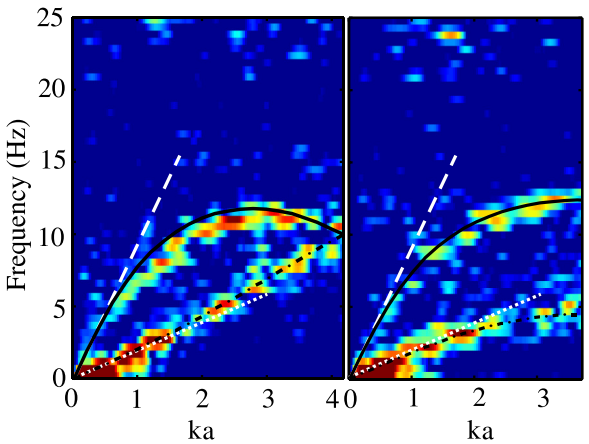

FIG. 3. (Color online) Fluctuation spectra of the in-plane particle velocity in a 2D plasma crystal. The spectra are for the two principal orientations of the lattice, $\theta = 0^\circ$ (left panel) and $\theta = 30^\circ$ (right panel). θ is defined as in Ref. [24]. The intensities of the spectra are in arbitrary units. The black solid (dash-dotted) lines are the theoretical dispersion relations of the longitudinal (transverse) waves computed with the parameters from Table I (last column). The white dashed (dotted) lines indicate the sound speeds of the longitudinal (transverse) waves; see Table I.

TABLE I. Plasma crystal parameters measured from the top- and side-view recording data as well as the parameter set adopted for numerical calculations.

Parameter	Top view	Side view	Theory
Lattice constant, a (μm)	520 ± 30[a]	530 ± 40[b]	500
Interaction range, κ	1.06		1.06
Particle charge, Q ($10^3 e$)	15.0 ± 2.3[c]		15.3
Vertical confinement parameter, f_v (Hz)	26 ± 3	24 ± 3	25
Longitudinal sound speed[d] (mm/s)	31.0 ± 2.2	32 ± 4	31
Transverse sound speed[d] (mm/s)	6.5 ± 1.2		6.5

[a]In the central part of the crystal, measuring $14.6 \times 14.6\,\mathrm{mm}^2$.
[b]Obtained from a row of particles that was well-aligned with the laser (left half of the top panel in Fig. 4).
[c]For the intralayer particles, assuming no decharging of particles by ion wakes.
[d]In-plane modes.

assures weak frictional coupling of the particle dynamics to the ambient gas. Therefore, the particle motion is not overdamped and studying of the naturally occurring waves (fluctuations) can give reliable information about the lattice layer. The experimentally measured fluctuation spectra of the in-plane particle velocity are shown in Fig. 3. The values of the particle charge Q, interaction range $\kappa = a/\lambda_D$ (where λ_D is the screening length), and the vertical confinement parameter f_v were estimated from the fluctuation spectra [41–43]. These parameters are collected in Table I along with the parameter set adopted for numerical calculations performed for comparison reasons.

The experimental fluctuation spectra of the out-of-plane particle velocity obtained from either the TV or SV recording systems are shown in Fig. 2. Although both methods are widely used in complex plasma experimental studies (see, e.g., Refs. [13,44] and the references therein), a cross-checking diagnostic has never been done before and the results of the TV and SV observations were never systematically compared. Below are important points of comparison that are worth to comment on: (i) the TV and SV spectra agree remarkably well with each other; (ii) the SV spectra show systematically lower resolution in the wave numbers due to a significantly poorer spatial sampling rate; (iii) the SV spectrum of the out-of-plane fluctuations is systematically lower (by about 0.5 Hz) than the TV spectrum most probably due to the fact that not exactly the same parts of the crystal are analyzed. It is also worth noting that the SV spectra are not angle-resolved [44]. A more detailed comparison is beyond the scope of the present research and will be reported elsewhere.

The electric field in the discharge (pre)sheath is inhomogeneous with the characteristic length given by

$$L_E = E_0/E_0' = g/(2\pi f_v)^2. \quad (1)$$

In our experimental conditions, $L_E \simeq 0.4\,\mathrm{mm}$; here, the balance

$$Z|e|E_0 = mg \quad (2)$$

is assumed to be valid. Note that a dense lattice layer, consisting of highly charged microparticles, itself produces a finite electric field in its vicinity. In our conditions it is not large, though, about one-fifth of E_0 in the mean-field approximation [45].

IV. DIRECT OBSERVATION OF THE INTERLAYER PARTICLE COLLISIONS

Upstream particles spontaneously moving above a 2D plasma crystal were reported for the first time in Ref. [8]. Their impact on the dynamics of the crystal layer and some aspects of particle coupling were studied. These fast-moving particles, even if they remain invisible (since they stay outside of the illuminating laser sheet), could be recognized by the appearance of the attraction-dominated Mach cones in the lattice, a signature uniquely manifesting their presence in an experiment. However, a direct observation of the particle-pairing process can only be done with the help of a side-view recording system, since the pairs tend to be extended in the vertical direction.

In our experiments, as in Ref. [8], a few upstream particles were wandering quasifreely on top of the lattice layer along the channels made by the rows of ordered intralayer particles. From time to time, encountering a lattice imperfection blocking the channel, they strongly scattered and were forced to change the track direction, then moved again quasifreely along another newly discovered path, and so on, covering a large area of the crystal. Usually, this process took quite a long time.

When an upstream particle happened to move in the vertical laser sheet, its trace was recorded by the side-view camera, as shown in Fig. 4. The travel path of an upstream particle is, on average, at the height of $\langle \Delta h \rangle \simeq 0.2\,\mathrm{mm} \simeq \frac{1}{2} L_E$ above the lattice layer (same as estimated in Ref. [8] using a top-view survey). In all cases shown in Fig. 4, the interaction scenario appears to be quite universal, passing normally through the following well-distinguished phases: initiation, repulsion, binding, and dragging. When an upstream particle comes too close to the channel wall or encounters a point defect, a strong interlayer collision between the top particle and a nearby intralayer one occurs. The bottom particle drops a little, allowing

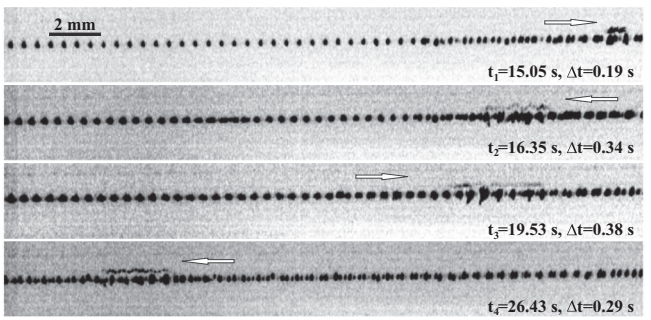

FIG. 4. Traces of the fast-moving upstream particles recorded by the side-view camera (a movie is available in the Supplemental Material [49]). Each panel was obtained by blending a sequence of snapshots; the recording timing is indicated [50]. The white arrows indicate the direction of motion of upstream particle. The apparent variation of the particle density across the image is due to the domain structure of the crystalline layer and its slow rotation. The illuminating laser light is coming from the left. Notice a small left grade (≈1%) of the main layer.

the "intruder" to pass over it. Then the repulsion is apparently replaced by attraction. The bottom particle starts to behave as if it was seized by the intruder, tending to be dragged with it. Since both particles are negatively charged, this is puzzling to some extent. The newly formed pair continues drifting for a while until the next strong collision would break it up.

V. COUPLED PAIRS AS QUASIPARTICLES

The association of two particles in a pair strongly affects the motion of both particles: They start to accelerate as if the momentum was not conserved during their collision; see Fig. 5. This kind of action-counteraction imbalance is not surprising at all, keeping in mind the following. First, the binding and subsequent dragging of an intralayer particle, the follower, actually is a direct manifestation of the ion focus (localized positive spatial charge or the ion wake) formed beneath the top particle, which is in the upstream position in the pair. A negatively charged bottom particle [47] is attracted by the ion focus while it is repelled by the negatively charged top particle [1,8]. At the same time, the bottom particle continues to repel the top one whence accelerating it [9]. The forces working to produce this motion are the plasma forces [48].

Newly formed pairs behave as *quasiparticles*, which are (roughly) double-charged compared to the individual particles in the monolayer. This helps them to permeate through the lattice and to find an optimal path, e.g., inside a channel formed by the lattice particles, as the example shown in Fig. 5 (right panel) demonstrates.

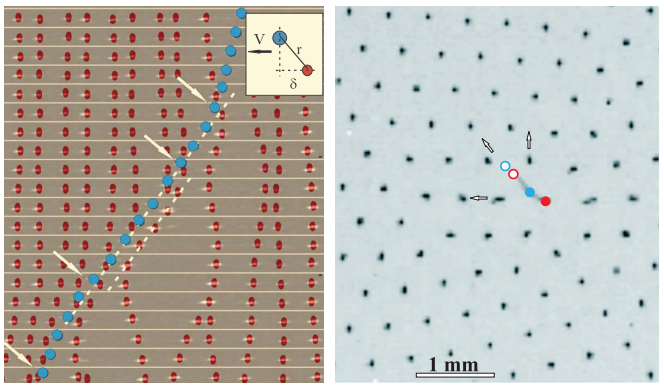

FIG. 5. (Color) Pairing of an upstream particle with intralayer particles. The left panel shows a space-time diagram assembled from 20 consecutive side-view images (each approximately $4.3 \times 0.8\,\mathrm{mm}^2$ in size). Time advances from top to bottom (in the range of 16.38–16.57 s; see Fig. 4), the time step is 0.009646 s. The cyan and red circles indicate the positions of, respectively, upstream and intralayer particles. The arrows indicate pairing events. The track of a long-living pair of particles (with a lifetime $\tau \simeq 0.05$ s) is highlighted by two parallel dashed lines. The inset shows the dragging geometry. The right panel shows the top view of a different dragging event (assembled from 15 blended images; here, the illuminating laser sheet was shifted upward, which allowed us to simultaneously record the upstream and intralayer particles). The filled circles indicate the positions of the upstream (cyan) and intralayer (red) particles in the beginning of a pairing event. The empty circles indicate the particle positions 0.06 s later. The arrows indicate the resultant directions of particle motion.

Upstream particles move nonuniformly along their trajectories. For instance, in Fig. 5 (left panel) the velocity of such a particle is about 7 mm/s in the beginning and in the end of the travel path. However, it is more than twice larger, $\langle V \rangle \simeq 18$ mm/s, when the particle becomes coupled, forming a close pair. This acceleration is due to the horizontal projection of the repulsion force between the coupled particles that is not completely canceled out. The average distance between the particles in the pair is $r \simeq 0.36$ mm, its horizontal projection (dragging distance) is $\delta \simeq 0.19$ mm. On average, the dragged particle in the pair is kept at the height $\langle \Delta h \rangle_{\mathrm{drag}} \approx 40\,\mu$m below the monolayer equilibrium position, experiencing therefore an extra force of external confinement. This gives a useful estimate of the z component of the interpair repulsion force pressing it down: $\langle F_z \rangle / mg = \langle \Delta h \rangle_{\mathrm{drag}} / L_E \approx 10\%$.

Given the approximately constant velocity of the pair, it is straightforward to roughly estimate the x component of the dragging force: $\langle F_x \rangle / mg \approx 2\gamma_E \langle V \rangle / g \simeq 0.4\%$. It is about 25 times weaker compared to the vertical z component, in good agreement with that measured in Ref. [8]. Following Refs. [27,51], the coupling between the particles in a pair can be conveniently interpreted through Hooke's spring constant. Introduced by the relationship $\langle F_x \rangle = k\delta$, where δ is the dragging distance, it is $k \approx 900\,\mathrm{eV/mm}^2$, noticeably well in line with that reported in Refs. [27,51]. The absolute value of the dragging force is $\langle F_x \rangle \approx 27$ fN for this particular example. In fact, it is less than the peak attractive interaction (60–230 fN) measured in argon at higher pressures [32], but larger than the value of 1.6 fN measured in helium [31].

VI. LIFETIME OF PARTICLE PAIRS

The particle pairs that spontaneously formed in plasma crystals in the course of our experiments were metastable. Their lifetime τ is an important parameter, which can give a hint on the mechanism of spontaneous formation and self-acceleration of particle pairs.

It is instructive to compare the lifetime τ of a particle pair with one period of vertical oscillations of the intralayer particles, f_v^{-1}. About 50% of all observed pairing events had a lifetime $\tau \lesssim f_v^{-1} \approx 0.04$ s. We classify these pairing events as short-term; see Fig. 6 (left panel) for examples. Pairing events with $\tau > f_v^{-1}$ can be regarded long-term. Examples are shown in Fig. 5 (left panel), where $\tau f_v \approx 1.3$, and in Fig. 6 (right panel), where $\tau f_v \approx 2$. Therefore, the lifetime of a particle pair is apparently not limited by the lattice vertical oscillations. The actual limiting factor may be strong in-plane collisions of the dragged intralayer component of the pair.

The pair formation time (as well as the decomposition time) is even shorter, about 0.01–0.02 s. Therefore, these processes are controlled by much stronger coupling forces producing accelerations of the order of 50–100 cm/s^2, according to our estimates. The driving force at this stage is about 300–600 fN. This force is of the order of the interparticle repulsion force,

$$F_{\mathrm{rep}} = Q_1 Q_2 \frac{1+\kappa r}{r^2} e^{-\kappa r}, \tag{3}$$

at typical distances $r = 0.2$–0.3 mm between the pair components. It is easy to check for our set of parameters from Table I, assuming that the particles are equally charged,

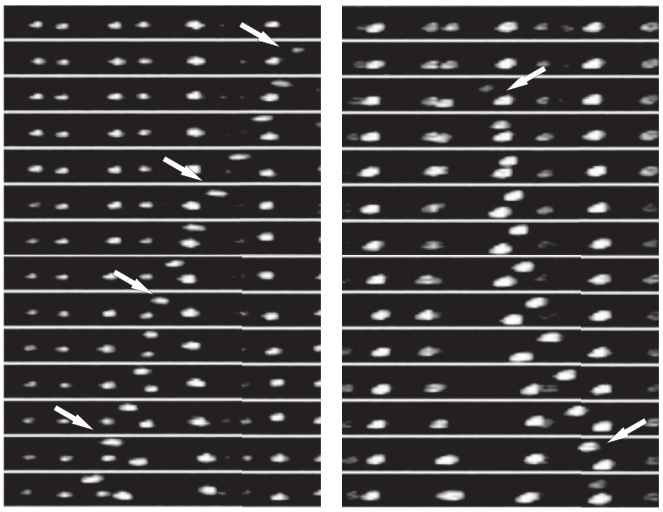

FIG. 6. Series of short-term coupling events (left panel) and a long-term coupling event (right panel) initiated by two different upstream particles in the course of the same experiment. Each panel is assembled from 14 consecutive side-view images (each approximately $3.9 \times 0.9\,\mathrm{mm}^2$ in size). Time advances from top to bottom; the time step is 0.009646 s. The upstream particles are clearly seen somewhat above the main layer. The white arrows indicate the starting points of pairing events.

$Q_1 \approx Q_2 \approx Q$. Note that the driving force at this stage is almost ten times stronger than that necessary for dragging.

Finally, we would like to discuss a somewhat different situation where particle pairs can live even longer. Figure 7 shows a side view of an upstream particle caged in a cell formed by lattice particles [52]. This configuration remained stable for at least 11.6 s; see Fig. 7(a). An instability set in at $t \simeq 11.6$–11.8 s, precipitated by a decrease in the distance between two cage particles from 0.86 ± 0.04 mm to 0.62 ± 0.04 mm. When the oscillation amplitude increased, the upstream particle, shifting rightwards, paired with the neighboring lattice particle for at least 0.1–0.14 s ($\tau f_v = 2.6$–3.6). Then it became invisible, probably leaving the illumination laser sheet transversally at $t = 12.5$ s.

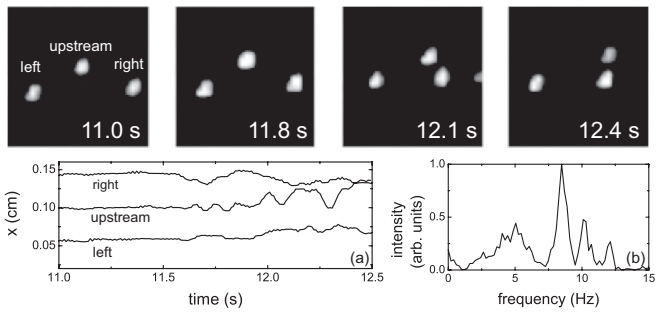

FIG. 7. Caged upstream particle. In the upper row, four configurations are shown from left to right: stable configuration, the onset of instability, and two pairing events. In all images, the field of view is $1.2 \times 1.2\,\mathrm{mm}^2$. Panel (a) shows the horizontal x projection of the particle positions as a function of time. The instability sets in at $t \simeq 11.6$–11.8 s. Panel (b) shows the fluctuation spectrum of the longitudinal oscillations of upstream particle.

The dominant frequency of the stable low-amplitude horizontal oscillations of the upstream particle is 8.4 ± 0.5 Hz; see Fig. 7(b). For the parameters from Table I, the horizontal "bouncing" frequency f_b of the caged upstream particle is

$$f_b = \frac{|Q|}{2\pi a}\sqrt{\frac{2}{ma}(2 + 2\kappa + \kappa^2)e^{-\kappa}} \simeq 8\ \mathrm{Hz}, \tag{4}$$

which is close to that observed. [A comparatively small correction $\propto (h/a)^2$ stemming from the finiteness of the height h above the monolayer can be neglected.]

The frequency of the low-amplitude vertical oscillations of the upstream particle is 25.8 ± 0.5 Hz, which is about 2 Hz higher than that of the cage particles, 23.8 ± 0.5 Hz. According to Eq. (1), the frequency increase corresponds to the proportional decrease of the electric field inhomogeneity length:

$$\frac{\Delta L_E}{L_E} = -2\frac{\Delta f_v}{f_v} \simeq 15\%. \tag{5}$$

We ascribe the enhanced inhomogeneity of the electric field to the nearby (charged) particle layer. In the mean-field approximation, it is given by

$$\frac{\Delta L_E}{L_E} \approx \frac{4\pi\kappa}{\sqrt{3}}\frac{Q^2 L_E}{mga^3} \simeq 20\%, \tag{6}$$

in fairly good agreement with experiment.

VII. CONCLUSION

We have observed for the first time the spontaneously forming mobile pairs of coupled particles in a 2D plasma crystal. This phenomenon is different from previously reported channeling [8] or "classical tunneling" [23]. This observation was made possible by combined top- and side-view imaging of the dust particle suspension. We argue that the apparent self-acceleration of a particle pair is a direct consequence of the plasma wake effect. These naturally occurring mobile pairs are metastable. They are, however, long-living enough for their reliable detection under our experimental conditions. The pairs we reported on in the present paper were formed by particles located initially at different heights. This helped us to initialize the pairing process, because the mutual wake-mediated interaction was easily activated in this case. It is not strictly necessary for the particles to be *initially* at different heights, though. The pairing of particles is also possible, for instance, in the experimental situations when their vertical displacement becomes relatively large, thus enhancing the mutual wake-mediated interaction. Particle pairing is of primary significance in experimental studies of the later stages of the wake-mediated melting [24], as our preliminary observations have demonstrated.

ACKNOWLEDGMENTS

This work was supported by the European Research Council under the European Union's Seventh Framework Programme (FP7/2007-2013)/ERC Grant No. 267499 and by the French-German PHC PROCOPE program (Project No. 28444XH).

[1] G. E. Morfill and A. V. Ivlev, Rev. Mod. Phys. **81**, 1353 (2009).

[2] V. E. Fortov, A. V. Ivlev, S. A. Khrapak, A. G. Khrapak, and G. E. Morfill, Phys. Rep. **421**, 1 (2005).

[3] H. Ikezi, Phys. Fluids **29**, 1764 (1986); H. Thomas, G. E. Morfill, V. Demmel, J. Goree, B. Feuerbacher, and D. Möhlmann, Phys. Rev. Lett. **73**, 652 (1994); Y. Hayashi and K. Tachibana, Jpn. J. Appl. Phys. **33**, L804 (1994); J. H. Chu and Lin I., Phys. Rev. Lett. **72**, 4009 (1994).

[4] H. M. Thomas and G. E. Morfill, Nature (London) **379**, 806 (1996); H. Thomas, G. E. Morfill, V. Demmel, J. Goree, B. Feuerbacher, and D. Möhlmann, Phys. Rev. Lett. **73**, 652 (1994).

[5] V. Nosenko, S. Zhdanov, and G. E. Morfill, Phys. Rev. Lett. **99**, 025002 (2007); V. Nosenko, S. Zhdanov, and G. Morfill, Phil. Mag. **88**, 3747 (2008).

[6] S. K. Zhdanov, M. H. Thoma, and G. E. Morfill, New J. Phys. **13**, 013039 (2011).

[7] The term "extra particle" was used in Ref. [9] for a particle moving about in a plane beneath a monolayer in what the authors termed an "incomplete lower layer."

[8] C.-R. Du, V. Nosenko, S. Zhdanov, H. M. Thomas, and G. E. Morfill, Europhys. Lett. **99**, 55001 (2012).

[9] V. A. Schweigert, I. V. Schweigert, A. Melzer, A. Homann, and A. Piel, Phys. Rev. E **54**, 4155 (1996); Phys. Rev. Lett. **80**, 5345 (1998); V. A. Schweigert, I. V. Schweigert, V. Nosenko, and J. Goree, Phys. Plasmas **9**, 4465 (2002).

[10] S. Nunomura, D. Samsonov, S. Zhdanov, and G. Morfill, Phys. Rev. Lett. **96**, 015003 (2006).

[11] D. Samsonov, J. Goree, Z. W. Ma, A. Bhattacharjee, H. M. Thomas, and G. E. Morfill, Phys. Rev. Lett. **83**, 3649 (1999); D. Samsonov, J. Goree, H. M. Thomas, and G. E. Morfill, Phys. Rev. E **61**, 5557 (2000).

[12] M. Schwabe, K. Jiang, S. Zhdanov, T. Hagl, P. Huber, A. V. Ivlev, A. M. Lipaev, V. I. Molotkov, V. N. Naumkin, K. R. Sütterlin, H. M. Thomas, V. E. Fortov, G. E. Morfill, A. Skvortsov, and S. Volkov, Europhys. Lett. **96**, 55001 (2011).

[13] L. Couëdel, D. Samsonov, C. Durniak, S. K. Zhdanov, H. M. Thomas, G. E. Morfill, and C. Arnas, Phys. Rev. Lett. **109**, 175001 (2012).

[14] M. Kretschmer, S. A. Khrapak, S. K. Zhdanov, H. M. Thomas, G. E. Morfill, V. E. Fortov, A. M. Lipaev, V. I. Molotkov, A. I. Ivanov, and M. V. Turin, Phys. Rev. E **71**, 056401 (2005).

[15] K. Combs, J. S. Olafsen, A. Burdeau, and P. Viot, Phys. Rev. E **78**, 042301 (2008).

[16] A. Patti, D. El Masri, R. van Roij, and M. Dijkstra, Phys. Rev. Lett. **103**, 248304 (2009).

[17] S. Ogata and S. Ichimaru, Phys. Rev. Lett. **62**, 2293 (1989); J. B. Pieper and J. Goree, *ibid.* **77**, 3137 (1996); K. Yang, *ibid.* **87**, 056802 (2001).

[18] M. F. Shlesinger, G. M. Zaslavsky, J. Klafter, and G. E. Morfill, Nature **363**, 31 (1993).

[19] M. Lampe, G. Joyce, G. Ganguli, and V. Gavrishchaka, Phys. Plasmas **7**, 3851 (2000).

[20] V. Steinberg, R. Sütterlin, A. V. Ivlev, and G. E. Morfill, Phys. Rev. Lett. **86**, 4540 (2001).

[21] A. Melzer, Plasma Sources Sci. Technol. **10**, 303 (2001).

[22] A. V. Ivlev, U. Konopka, G. E. Morfill, and G. Joyce, Phys. Rev. E **68**, 026405 (2003).

[23] G. E. Morfill, U. Konopka, M. Kretschmer, M. Rubin-Zuzic, H. M. Thomas, S. K. Zhdanov, and V. Tsytovich, New J. Phys. **8**, 7 (2006).

[24] L. Couëdel, V. Nosenko, S. K. Zhdanov, A. V. Ivlev, H. M. Thomas, and G. E. Morfill, Phys. Rev. Lett. **103**, 215001 (2009).

[25] M. Kroll, J. Schablinski, D. Block, and A. Piel, Phys. Plasmas **17**, 013702 (2010).

[26] J. Kong, T. W. Hyde, L. Matthews, K. Qiao, Z. Zhang, and A. Douglass, Phys. Rev. E **84**, 016411 (2011).

[27] L. Wörner, C. Räth, V. Nosenko, S. K. Zhdanov, H. M. Thomas, G. E. Morfill, J. Schablinski, and D. Block, Europhys. Lett. **100**, 35001 (2012).

[28] L. N. Cooper, Am. J. Phys. **28**, 91 (1960).

[29] P. K. Shukla and N. N. Rao, Phys. Plasmas **3**, 1770 (1996).

[30] D. P. Resendes, J. T. Mendoca, and P. K. Shukla, Phys. Lett. A **239**, 181 (1998).

[31] A. Melzer, V. A. Schweigert, and A. Piel, Phys. Rev. Lett. **83**, 3194 (1999).

[32] G. A. Hebner and M. E. Riley, Phys. Rev. E **68**, 046401 (2003).

[33] G. A. Hebner, M. E. Riley, and B. M. Marder, Phys. Rev. E **68**, 016403 (2003).

[34] M. E. Markes and P. F. Williams, Phys. Lett. A **278**, 152 (2000).

[35] J. Kong, T. W. Hyde, and J. Carmona-Reyes, IEEE Trans. on Plasma Sci. **36**, 554 (2008).

[36] A. A. Samarian and S. V. Vladimirov, Contrib. Plasma Phys. **49**, 260 (2009).

[37] V. Nosenko, A. V. Ivlev, S. K. Zhdanov, M. Fink, and G. E. Morfill, Phys. Plasmas **16**, 083708 (2009).

[38] S. S. Rogers, T. A. Waigh, X. Zhao, and J. R. Lu, Phys. Biol. **4**, 220 (2007).

[39] J. D. Williams, E. Thomas, Jr., L. Couëdel, A. V. Ivlev, S. K. Zhdanov, V. Nosenko, H. M. Thomas, and G. E. Morfill, Phys. Rev. E **86**, 046401 (2012).

[40] P. S. Epstein, Phys. Rev. **23**, 710 (1924).

[41] S. K. Zhdanov, A. V. Ivlev, and G. E. Morfill, Phys. Plasmas **16**, 083706 (2009).

[42] S. Nunomura, J. Goree, S. Hu, X. Wang, A. Bhattacharjee, and K. Avinash, Phys. Rev. Lett. **89**, 035001 (2002).

[43] S. Zhdanov, S. Nunomura, D. Samsonov, and G. E. Morfill, Phys. Rev. E **68**, 035401(R) (2003).

[44] B. Liu, J. Goree, and Y. Feng, Phys. Rev. Lett. **105**, 085004 (2010); **105**, 269901 (2010).

[45] H. Totsuji, C. Totsuji, and K. Tsuruta, Phys. Rev. E **64**, 066402 (2001).

[46] D. Samsonov, S. Zhdanov, and G. E. Morfill, Phys. Rev. E **71**, 026410 (2005).

[47] Note that the charge of the lower particle in a pair is not the same as for the intralayer particles due to decharging of particles by ion wakes; see, e.g., J. Carstensen, F. Greiner, L.-J. Hou, H. Maurer, and A. Piel, Phys. Plasmas **16**, 013702 (2009).

[48] S. K. Zhdanov, A. V. Ivlev, and G. E. Morfill, Phys. Plasmas **12**, 072312 (2005).

[49] See Supplemental Material at http://link.aps.org/supplemental/10.1103/PhysRevE.89.023103 for examples of particle pairing. The experimental movie was recorded at 103.7 fps and converted into MPEG-4 format at a frame rate of 25 fps.

[50] The standard blend function of Mathcad 14.0 was used. Blending is useful in subtracting and rebiasing backgrounds.

[51] M. A. Fink, S. K. Zhdanov, M. H. Thoma, H. Höfner, and G. E. Morfill, Phys. Rev. E **86**, 065401(R) (2012).

[52] Caged upstream particles are sometimes recorded even in the top-view images of 2D complex plasmas when the illuminating laser sheet is set somewhat higher than the main layer (sometimes on purpose [8,24]).